

# Weak localization and conductance fluctuations in a quantum dot with parallel magnetic field and spin-orbit scattering

Jan-Hein Cremers

*Lyman Laboratory of Physics, Harvard University, Cambridge MA 02138*

Piet W. Brouwer

*Laboratory of Atomic and Solid State Physics, Cornell University, Ithaca, NY 14853-2501*

Vladimir I. Fal'ko

*Physics Department, Lancaster University, Lancaster LA1 4YB, United Kingdom*

(Dated: November 20, 2018)

In the presence of both spin-orbit scattering and a magnetic field the conductance of a chaotic GaAs quantum dot displays quite a rich behavior. Using a Hamiltonian derived by Aleiner and Fal'ko [Phys. Rev. Lett. **87**, 256801 (2001)] we calculate the weak localization correction and the covariance of the conductance, as a function of parallel and perpendicular magnetic field and spin-orbit coupling strength. We also show how the combination of an in-plane magnetic field and spin-orbit scattering gives rise to a component to the magnetoconductance that is anti-symmetric with respect to reversal of the perpendicular component of the magnetic field and how spin-orbit scattering leads to a “magnetic-field echo” in the conductance autocorrelation function. Our results can be used for a measurement of the Dresselhaus and Bychkov-Rashba spin-orbit scattering lengths in a GaAs/GaAlAs heterostructure.

PACS numbers: 73.23.-b, 05.45.Mt, 72.20.My, 73.63.Kv

## I. INTRODUCTION

A two-dimensional (2D) electron gas offers ample opportunity for manipulation of the electron's spin and orbital state. In the absence of spin-orbit coupling, such manipulation can be performed separately on the electron spin and orbital degree of freedom, by means of magnetic fields of various orientations and electrostatic gates. On one hand, a magnetic field parallel to the plane of the 2D gas lifts the spin degeneracy and allows for a measurement that distinguishes between the transport properties of “up” and “down” spins: As long as the confining potential that determines the 2D electron gas is sharp, it does not significantly affect the electron's orbital degrees of freedom. On the other hand, gate voltages and a weak magnetic field perpendicular to the quantum well act on the orbital degrees of freedom and do not couple significantly to the electron's spin.<sup>1</sup>

Spin-orbit scattering couples the spin and orbital degrees of freedom. Conventionally, the main signature of spin-orbit coupling in the 2D electron gas in GaAs heterostructures is the observation of weak anti-localization, a small positive quantum correction to the conductivity that is suppressed by a magnetic field.<sup>2</sup> Weak anti-localization is the counterpart of weak localization, a negative correction to the conductivity at zero magnetic field caused by the constructive interference of back-scattered electron waves in a phase-coherent disordered conductor in the absence of spin-orbit scattering.<sup>3</sup> Only recently, spin-dependent phase coherent transport was considered for a quantum dot, a small island of the electron gas confined by gates<sup>4</sup>. Motivated by an experiment by Folk *et al.*,<sup>5</sup> theoretical works by Halperin *et al.*<sup>6</sup> and by two

of the authors,<sup>7</sup> have shown that the combination of spin-orbit scattering and a spin degeneracy lifting parallel magnetic field leads to a remarkably rich structure of quantum interference phenomena in III-V semiconductor quantum dots, that far surpasses a simple interpolation between weak localization and weak antilocalization physics.

Not only does the crossover regime between weak localization and anti-localization represent an interesting issue of its own, understanding features imposed upon quantum transport by spin-orbit coupling is needed for a correct extraction of the decoherence time from experimental data. For electrons in a small dot with weak but finite spin-orbit coupling, the the crossover of weak localization to anti-localization manifests itself as a suppression of the zero-temperature value of localization correction to the dot conductance. This suppression of the weak localization correction may be misinterpreted as a saturation of the decoherence time  $\tau_\phi$  at low temperatures. Without a priori knowledge of the spin-orbit coupling constants for a given semiconductor dot, one must use the features of spin-orbit coupling induced interference effects in order to identify the origin of what can be mistaken for a suppression of the interference part of conductance, when the observed weak localization correction is less than the prediction of the quantum transport theory for to the crossover between orthogonal and unitary symmetry classes.

In this publication, we present a detailed quantitative analysis of the influence of the coupling between electron spin and orbital motion in a two-dimensional semiconductor on the interference corrections to the conductance of a quantum dot. We consider the effects of en-

hanced/suppressed back-scattering and the variance and correlation properties of universal conductance fluctuations. The calculations, which are performed in the framework of the random scattering matrix approach of random matrix theory, are described in Sections III and IV. In Section III, we present the analysis of the average conductance of a chaotic dot, Section IV is devoted to conductance fluctuations. For technical reasons, we limit our attention to the case of a large number of channels,  $N_1$  and  $N_2$  in the point contact connecting the dot to the bulk, though all qualitative features we discover for  $N \gg 1$  would persist in the case of  $N \sim 1$ . These two technical sections are preceded by a qualitative discussion (Sec. II) and followed by an analysis of the effect of a spatially non-uniform spin-orbit coupling strength (Sec. V).

## II. INTERPLAY BETWEEN SO COUPLING AND ZEEMAN SPLITTING IN QUANTUM DOTS

In GaAs/AlGaAs heterostructures, spin-orbit coupling owes its existence to the asymmetry of the potential confining the 2DEG and the lack of inversion symmetry in the crystal structure, leading to the Bychkov-Rashba and Dresselhaus terms in the Hamiltonian. In the theory we present below, we consider electrons in a heterostructure or quantum well lying in the (001) crystallographic plane of a zinc-blend type semiconductor and choose coordinates  $x_1, x_2$  along crystallographic directions  $\hat{\mathbf{e}}_1 = [110]$  and  $\hat{\mathbf{e}}_2 = [1\bar{1}0]$  (coordinate  $x_3$  is perpendicular to the plane of the two-dimensional electron gas). The effective two-dimensional Hamiltonian of electrons in a quantum dot takes the form

$$\mathcal{H} = \frac{1}{2m} \left[ \left( p_1 - eA_1 - \frac{\sigma_2}{2\lambda_1} \right)^2 + \left( p_2 - eA_2 + \frac{\sigma_1}{2\lambda_2} \right)^2 \right] + V(\mathbf{r}) + \frac{1}{2} \mu_B g \mathbf{B} \cdot \boldsymbol{\sigma}. \quad (1)$$

where  $\mathbf{B}$  is the magnetic field,  $\mathbf{A} = B_3(\hat{\mathbf{e}}_3 \times \mathbf{r})/2c$  is the vector potential corresponding to the component of the magnetic field perpendicular to the plane of the two-dimensional electron gas, and  $\boldsymbol{\sigma} = (\sigma_1, \sigma_2, \sigma_3)$  the vector of Pauli matrices. The potential  $V$  both confines the electrons to the quantum dot and describes elastic scattering from non-magnetic impurities in the dot. The two length scales,  $\lambda_1$  and  $\lambda_2$  are associated with spin-orbit coupling for an electron moving along the principal crystallographic directions  $\hat{\mathbf{e}}_1$  and  $\hat{\mathbf{e}}_2$ ,<sup>8</sup> and characterize the length at which spin of an initially polarized electron would precess with an angle  $2\pi$ .

For a dot with homogeneous electron density and, therefore, parameters of confining potential, spin-orbit coupling parameters  $\lambda_1$  and  $\lambda_2$  are independent of the position. In that case, the spin-orbit coupling takes the form of a spin-dependent "vector potential", which is

non-abelian since the Pauli matrices do not commute with each other.<sup>9,10,11</sup> If  $\lambda_1$  and  $\lambda_2$  are large compared to the dot size  $L$ , the non-commutativity of this spin-dependent vector potential involves higher powers of  $L/\lambda_{1,2}$ , so that the spin-orbit coupling can be "gauged out" to leading order in  $L/\lambda_{1,2}$ . This may be achieved through the unitary transformation  $\psi(\mathbf{r}) = U(\mathbf{r})\tilde{\psi}(\mathbf{r})$ ,

$$U = \exp\left(\frac{ix_1\sigma_2}{2\lambda_1} - \frac{ix_2\sigma_1}{2\lambda_2}\right) = \cos R + \left(\frac{ix_1\sigma_2}{2\lambda_1} - \frac{ix_2\sigma_1}{2\lambda_2}\right) \frac{\sin R}{R}, \quad (2)$$

$$R = \sqrt{\left(\frac{x_1}{2\lambda_1}\right)^2 + \left(\frac{x_2}{2\lambda_2}\right)^2}, \quad (3)$$

which performs a position-dependent rotation of the spin out of the plane of the two-dimensional electron gas to the locally adjusted frame.<sup>7</sup> Below, we assume that  $R \ll 1$ , and use  $R$  as a small parameter to derive the form of the Hamiltonian  $\tilde{\mathcal{H}} = U^\dagger \mathcal{H} U$  in the locally rotated spin-frame,

$$\tilde{\mathcal{H}} = \frac{1}{2m} (-i\hbar\nabla - e\mathbf{A} - \mathbf{a}_\perp - \mathbf{a}_\parallel)^2 + h^Z + h_\perp^Z + V(\mathbf{r}). \quad (4)$$

Here we introduced the spin-dependent vector potential

$$\mathbf{a}_\perp = \frac{\sigma_3}{4\lambda_1\lambda_2} [\hat{\mathbf{e}}_3 \times \mathbf{r}]$$

that has the same form as a magnetic field  $\pm ec\hat{\mathbf{e}}_3/2\lambda_1\lambda_2$  with opposite directions for electrons with spins "up" and "down" in the new spin-frame, and we also abbreviated

$$\begin{aligned} \mathbf{a}_\parallel &= \frac{1}{6\lambda_1\lambda_2} \left( \frac{x_1\sigma_1}{\lambda_1} + \frac{x_2\sigma_2}{\lambda_2} \right) [\hat{\mathbf{e}}_3 \times \mathbf{r}] \\ h^Z &= \frac{1}{2} \mu_B g \mathbf{B} \cdot \boldsymbol{\sigma}, \\ h_\perp^Z &= -\mu_B g \left( \frac{B_1 x_1}{2\lambda_1} + \frac{B_2 x_2}{2\lambda_2} \right) \sigma_3. \end{aligned} \quad (5)$$

The Hamiltonian (4) describes electrons in a rotated spin frame. It contains all relevant terms that lift the high degree of symmetry of a system with uncoupled orbital and spin degrees of freedom, to leading order in the small parameter  $L/\lambda_{1,2}$ . In these equations, we omitted sub-leading terms of higher order in  $L/\lambda_{1,2}$  that do not affect the symmetry of the Hamiltonian.

As long as the rate at which electrons escape from the quantum dot into the leads is much smaller than the Thouless energy  $E_{\text{Th}}$ , transport properties of the quantum dot can be calculated using random matrix theory.<sup>12</sup> The use of random matrix theory requires an analysis of the symmetries of the scattering matrix, which are set by the relative magnitudes of characteristic energy scales for each of the terms in the Hamiltonian (4) and the escape

rate. These energy scales are

$$\begin{aligned}
\varepsilon_B &= \kappa E_{\text{Th}} (eB_3 L^2 / 2\hbar)^2, \\
\varepsilon_{\perp}^{\text{so}} &= \kappa E_{\text{Th}} (L^2 / 4\lambda^2)^2, \\
\varepsilon_{\parallel}^{\text{so}} &= \kappa' (L^2 / 4\lambda^2) \varepsilon_{\perp}^{\text{so}}, \\
\varepsilon^Z &= \mu_B g B, \\
\varepsilon_{\perp}^Z &= \frac{\kappa'' (\varepsilon^Z)^2}{E_{\text{Th}}} (L^2 / 4\lambda^2),
\end{aligned} \tag{6}$$

for the orbital contribution of the magnetic field, the spin-orbit terms  $a_{\parallel}$  and  $a_{\perp}$ , and the Zeeman coupling terms  $h^Z$  and  $h_{\perp}^Z$ , respectively. For weak uniform spin-orbit coupling in a small dot such that  $L/\lambda_{1,2} \ll 1$ , one has the strong inequalities

$$\varepsilon_{\parallel}^{\text{so}} \ll \varepsilon_{\perp}^{\text{so}}, \quad \varepsilon_{\perp}^Z \ll \varepsilon^Z. \tag{7}$$

Here  $E_{\text{Th}}$  is the Thouless energy, which is the largest energy scale in the problem,  $\lambda^2 = \lambda_1 \lambda_2$ , and  $\kappa$ ,  $\kappa'$ , and  $\kappa''$  are coefficients of order unity. The coefficients  $\kappa'$  and  $\kappa''$  depend on the sample geometry and on the ratio  $\lambda_1/\lambda_2$  of the spin-orbit lengths. The coefficient  $\kappa''$  also depends on the direction of the magnetic field. The coefficient  $\kappa$  depends on the sample geometry only; it appears both for the orbital contribution of the magnetic field and for the spin-orbit term  $a_{\perp}$  because both terms have the same spatial dependence. For a circular quantum dot with radius  $L$ , mean free path  $l \ll L$ , Fermi velocity  $v_F$ , and  $\lambda_1 = \lambda_2 = \lambda$ , one has  $E_{\text{Th}} = \hbar v_F l / 2L^2$ ,  $\kappa = 2$ ,  $\kappa' = 1/3$  and  $\kappa'' \approx 0.292$ , see App. A.

If the spin-orbit coupling is non-uniform, i.e., when the spin-orbit lengths  $\lambda_1$  and  $\lambda_2$  depend on position, the ‘‘spin-dependent vector potential’’ in Eq. (1) can no longer be gauged away to leading order in  $L/\lambda_{1,2}$ . A spatially non-uniform spin-orbit coupling can be created intentionally, with the help of a metal gate parallel to the two-dimensional electron gas that changes the asymmetry of the quantum well.<sup>13,14,15</sup> or arise as a by-product of the confining gates. Generically, the non-uniformity gives rise to a term in the Hamiltonian of the same symmetry as  $\mathbf{a}_{\parallel}$  in Eq. (4).<sup>16</sup> Hence, the main effect of non-uniformities is to increase the corresponding energy scale  $\varepsilon_{\parallel}^{\text{so}}$  by an amount of order  $E_{\text{Th}}(L/\lambda_{\text{fl}})^2$ , where  $1/\lambda_{\text{fl}}$  is a measure of the fluctuations of the spin-orbit coupling  $\lambda_{1,2}^{-1}$ .<sup>16</sup> For very small quantum dots, this increase of  $\varepsilon_{\parallel}^{\text{so}}$  may eventually reverse the first inequality in Eq. (7).

It is the existence of two energy scales each to describe the strength of the spin-orbit and Zeeman terms in the Hamiltonian that leads to the rich parameter dependence of the conductance distribution of a chaotic quantum dot. When all relevant energy scales are either much larger or much smaller than the escape rate, the scattering matrix has a well defined symmetry, and the conductance distribution can be found using symmetry considerations alone.<sup>7</sup> It is the goal of this paper to address the general parameter regime, where an interpolation between the various symmetry classes is called for. Our results

are important for a quantitative analysis of recent experiments by Zumbühl *et al.*,<sup>15</sup> and for the development of techniques for experimental determination of spin-orbit coupling parameters. Looking into various regimes, we show how to extract such information from (a) weak localization measurements in the presence of an in-plane magnetic field; (b) an analysis of how the in-plane magnetic field gives rise to a component of the magnetoconductance that is anti-symmetric in the perpendicular magnetic field; and (c) from the possible observation of a ‘‘magnetic field echo’’ in the auto-correlation function of conductance fluctuations.

The latter prediction is made on the basis of the following theoretical observation. After the unitary transformation (2), the leading spin-orbit term  $\mathbf{a}_{\perp}^{\text{so}}$  has precisely the same spatial dependence as the vector potential due to the orbital magnetic field (in a symmetric gauge). Hence,  $\mathbf{a}_{\perp}^{\text{so}}$  can be regarded as an effective magnetic field perpendicular to the plane of the quantum well and of opposite sign for the two spin directions. A suitably chosen orbital magnetic field can balance this effective field, or change its sign for one spin direction, leading to a partial re-appearance of weak localization and to a ‘‘magnetic field echo’’ in the auto-correlation function of conductance fluctuations. The magnetic field echo appears in the magnetoconductance autocorrelation function for a magnetic field difference

$$\Delta B_3 = \frac{\hbar}{e\lambda_1\lambda_2}; \tag{8}$$

The shift of weak localization peaks is by half this field strength.

According to the Onsager’s relations, the two-terminal conductance of a non-magnetic system is symmetric with respect to reversal of the magnetic field  $\mathbf{B}$ . In the absence of spin-orbit coupling, the symmetry with respect to the reversal of the perpendicular magnetic field component  $B_3$  would persist even in the presence of Zeeman splitting caused in a 2D electron gas by the in-plane magnetic field  $\mathbf{B}_{\parallel}$  (excluding effects arising from the finite width of the quantum well.<sup>17</sup>) However, in the presence of even a weak SO coupling, the exact symmetry exists only if both  $B_3$  and  $B_{\parallel}$  are reversed simultaneously, whereas the reversal of the perpendicular component only generates an antisymmetric contribution to the magnetoconductance with variance

$$\text{var} [G(B_3, B_{\parallel}) - G(-B_3, B_{\parallel})] \sim \frac{(\varepsilon^Z)^2 \varepsilon_{\parallel}^{\text{so}}}{(N\Delta/2\pi)^3} \left(\frac{e^2}{\hbar}\right)^2, \tag{9}$$

where  $N$  is the number of channels in the leads,  $\Delta$  is the mean level spacing in the dot, and  $\langle G \rangle$  is the ensemble-averaged conductance of the quantum dot. Since the fluctuating antisymmetric contribution to the conductance,  $G(B_3, B_{\parallel}) - G(-B_3, B_{\parallel})$  is linear in the in-plane magnetic field,  $\varepsilon^Z \approx g\mu_B B_{\parallel}$ , it dominates over the conductance asymmetry caused by inter-subband mixing due to the

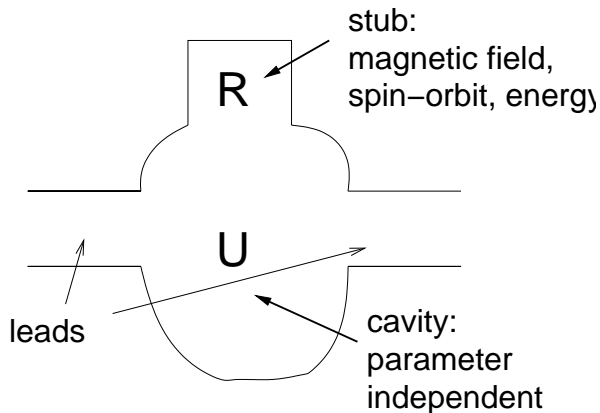


FIG. 1: Illustration of the quantum dot with stub. Energy dependent scattering from the quantum dot in the presence of spin-orbit coupling and a magnetic field is modeled as scattering from a chaotic quantum dot with a parameter independent scattering matrix  $U$ , with a stub described by a reflection matrix  $R$  which depends on energy, spin-orbit coupling and the magnetic field.

in-plane magnetic field for intermediate magnetic field strengths,<sup>17</sup> which is proportional to  $B_{\parallel}^3$ .

### III. AVERAGE CONDUCTANCE

The starting point of our calculation is the Landauer formula for the two-terminal conductance  $G$  of the quantum dot at zero temperature,

$$G = \frac{2e^2}{h} \frac{N_1 N_2}{N} - \frac{e^2}{h} \text{tr} S \Lambda S^\dagger \Lambda, \quad (10)$$

where the diagonal matrix  $\Lambda$  has elements

$$\Lambda_{jj} = \begin{cases} N_2/N, & j = 1, \dots, N_1, \\ -N_1/N, & j = N_1 + 1, \dots, N. \end{cases} \quad (11)$$

As a matrix of complex numbers, the scattering matrix  $S$  has dimension  $2N = 2(N_1 + N_2)$ ; it may also be seen as an  $N \times N$  matrix of quaternions, which are  $2 \times 2$  matrices with special rules for complex conjugation and transposition.<sup>18</sup>

In order to calculate the average of the conductance at Fermi energy  $\varepsilon$  and magnetic field  $\mathbf{B}$ , or the covariance at energies  $\varepsilon$  and  $\varepsilon'$  and magnetic fields  $\mathbf{B}$  and  $\mathbf{B}'$ , it is sufficient to compute the average

$$\langle S_{kl;\mu\nu}(\varepsilon, \mathbf{B}) S_{k'\nu';\mu'\nu'}(\varepsilon', \mathbf{B}')^* \rangle, \quad (12)$$

where roman indices refer to the propagating channels in the leads, and Greek indices refer to spin. Hereto, we need a statistical description of the scattering matrix  $S$  in the presence of spin-orbit scattering and for arbitrary values of the magnetic field  $\mathbf{B}$  and Fermi energy  $\varepsilon$ . Within the “random scattering matrix approach” of random-matrix theory, this is provided by the “stub

model”.<sup>19</sup> In this model, a fictitious “stub” is attached to the quantum dot, see Fig. 1. If the number of channels in the stub is  $M - N$ , the scattering matrix  $S$  can be written

$$S = PU(1 - Q^\dagger RQU)^{-1}P^\dagger, \quad (13)$$

where  $U$  is the  $M \times M$  scattering matrix of the quantum dot (without stub),  $R$  is the  $(M - N)$ -dimensional reflection matrix of the stub, and  $P$  and  $Q$  are  $N \times M$  and  $(M - N) \times M$  projection matrices, respectively, with  $P_{ij} = \delta_{i,j} \mathbb{1}$ , and  $Q_{ij} = \delta_{i+N,j} \mathbb{1}$ . (Here  $\mathbb{1}$  is the  $2 \times 2$  unit matrix in spin space.) The area and width of the stub are chosen such that (i) the dwell time in the stub is much larger than the dwell time in the quantum dot and (ii) the time for ergodic exploration of the dot plus stub system is much shorter than the time for escape into one of the two leads. The first condition ensures that all dependence on Fermi energy, magnetic field, or spin-orbit scattering rate will be through the reflection matrix  $R$ , so that the matrix  $U$  can be taken at a fixed reference energy  $\varepsilon = 0$  and at zero magnetic field and spin-orbit scattering rate. Since scattering from the quantum dot is chaotic, this implies that elements of  $U$  are proportional to the  $2 \times 2$  unit matrix in spin space  $\mathbb{1}$  and that  $U$  can be chosen from Dyson’s circular orthogonal ensemble of random matrix theory.<sup>12</sup> The second condition, which requires  $M \gg N$ , ensures that electrons explore the phase space of the combined dot plus stub system ergodically before they exit to the leads, so that the distribution of the scattering matrix  $S$  remains universal and is unaffected by the addition of the stub. Indeed, the parametric dependence of the scattering matrix described by the stub model has been shown to be the same as that described by the Hamiltonian approach of random-matrix theory.<sup>19</sup>

We take the reflection matrix  $R$  of the form

$$R = \exp \left[ \frac{2\pi i}{M\Delta} (\varepsilon - \mathcal{H}') \right], \quad (14)$$

where  $\Delta$  is the mean level spacing of the closed dot and  $\mathcal{H}'$  is an  $(M - N)$  dimensional matrix which describes the effect of the magnetic field and spin-orbit scattering,

$$\mathcal{H}' = \frac{\Delta}{2\pi} [i\mathcal{X}(x\mathbb{1} + a_{\perp}\sigma_3) + ia(\mathcal{A}_1\sigma_1 + \mathcal{A}_2\sigma_2) - \mathbf{b} \cdot \boldsymbol{\sigma} + b_{\perp}\mathcal{B}_h\sigma_3]. \quad (15)$$

Here  $\mathcal{X}$ ,  $\mathcal{A}_1$  and  $\mathcal{A}_2$  are real antisymmetric matrices, with  $\langle \text{tr} \mathcal{X} \mathcal{X}^T \rangle = M^2$  and  $\langle \text{tr} \mathcal{A}_i \mathcal{A}_j^T \rangle = \delta_{ij} M^2$ , while  $\mathcal{B}_h$  is a real symmetric matrix with  $\langle \text{tr} \mathcal{B}_h^2 \rangle = M^2$ . The dimensionless parameters  $x$ ,  $a_{\perp}$ ,  $a$ ,  $b$ , and  $b_{\perp}$  correspond to the energy scales defined in Eq. (6) as

$$\begin{aligned} x^2 &= \pi\varepsilon_B/\Delta, \\ a_{\perp}^2 &= \pi\varepsilon_{\perp}^{\text{SO}}/\Delta, \\ a^2 &= \pi\varepsilon_{\parallel}^{\text{SO}}/\Delta, \\ b &= \pi\varepsilon^Z/\Delta, \\ b_{\perp}^2 &= \pi\varepsilon_{\perp}^Z/\Delta. \end{aligned} \quad (16)$$

We define the corresponding quantities  $x'$ ,  $b'$ , and  $b'_\perp$  when calculating a correlator between scattering matrix elements at different values  $\mathbf{B}$  and  $\mathbf{B}'$  of the magnetic field. For weak uniform spin-orbit scattering, one has the strong inequalities  $a \ll a_\perp$ ,  $b_\perp \ll b$ .

To calculate the correlator (12), we expand  $S$  in powers of  $U$  using Eq. (13) and integrate  $U$  over the space of unitary symmetric matrices using the diagrammatic technique of Ref. 20. To leading order in  $1/M$  and  $1/N$  we can take the elements of  $U$  to be Gaussian random variables with mean zero and with variance  $\langle U_{ij}U_{kl}^* \rangle = M^{-1}(\delta_{ik}\delta_{jl} + \delta_{il}\delta_{jk})$ . Then only ladder diagrams and maximally crossed diagrams contribute to the correlator Eq. (12). Summing the contributions from these two classes of diagrams yields

$$\langle S_{kl;\mu\nu}(\varepsilon, \mathbf{B})S_{k'l';\mu'\nu'}^*(\varepsilon', \mathbf{B}') \rangle = \delta_{kk'}\delta_{ll'}D_{\mu\nu;\mu'\nu'} + \delta_{kl'}\delta_{lk'}(\mathcal{TCT})_{\mu\nu;\mu'\nu'}, \quad (17)$$

where

$$\begin{aligned} D &= (M\mathbb{1} \otimes \mathbb{1} - \text{tr} R \otimes R'^\dagger)^{-1}, \\ C &= (M\mathbb{1} \otimes \mathbb{1} - \text{tr} R \otimes R'^*)^{-1}. \end{aligned} \quad (18)$$

Here  $R'$  is given by Eq. (14), with  $x$ ,  $b$ ,  $b_\perp$  and  $\varepsilon$  replaced by  $x'$ ,  $b'$ ,  $b'_\perp$  and  $\varepsilon'$ , respectively. The superscript  $*$  denotes the quaternion complex conjugate of  $R'$ ,  $\mathcal{T} = \mathbb{1} \otimes \sigma_2$ , and the trace is taken over the channel indices only. The tensor multiplication in Eq. (18) has a reverse-order multiplication for the Pauli matrices in second place,

$$(\sigma_i \otimes \sigma_j)(\sigma_{i'} \otimes \sigma_{j'}) = (\sigma_i \sigma_{i'}) \otimes (\sigma_j \sigma_{j'}). \quad (19)$$

The two contributions  $C$  and  $D$  are the equivalents of cooperon and diffuson in the conventional diagrammatic perturbation theory.<sup>21</sup> Taking the limit  $M \rightarrow \infty$  and using Eq. (14) we find

$$\begin{aligned} D^{-1} &= N\mathbb{1} \otimes \mathbb{1} + \frac{2\pi i(\varepsilon - \varepsilon')}{\Delta} \mathbb{1} \otimes \mathbb{1} \\ &+ \frac{1}{2}[(x - x')\mathbb{1} \otimes \mathbb{1} + a_\perp(\sigma_3 \otimes \mathbb{1} - \mathbb{1} \otimes \sigma_3)]^2 \\ &+ \frac{1}{2}a^2(\sigma_1 \otimes \mathbb{1} - \mathbb{1} \otimes \sigma_1)^2 \\ &+ \frac{1}{2}a^2(\sigma_2 \otimes \mathbb{1} - \mathbb{1} \otimes \sigma_2)^2 \\ &+ i\mathbf{b} \cdot (\boldsymbol{\sigma} \otimes \mathbb{1} - \mathbb{1} \otimes \boldsymbol{\sigma}) \\ &+ \frac{1}{2}(h\sigma_3 \otimes \mathbb{1} - h'\mathbb{1} \otimes \sigma_3)^2. \end{aligned} \quad (20)$$

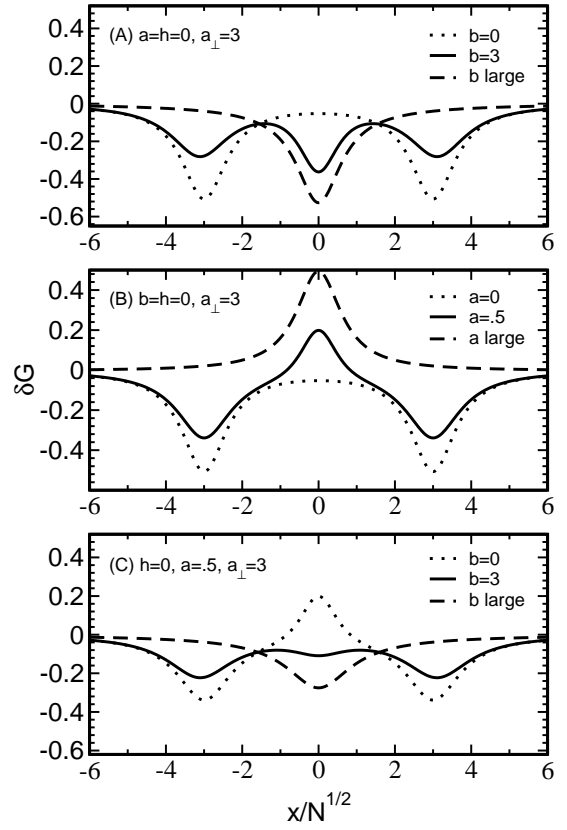


FIG. 2: Dependence of the quantum-interference correction to the conductance,  $\delta G$ , on the perpendicular magnetic field  $x$ . The conductance is measured in units of  $(2e^2/h)N_1N_2/(N_1 + N_2)^2$ . Panel (a) shows  $\delta G$  for  $a_\perp = 3$ ,  $a = 0$ ,  $b_\perp = 0$  and two values of the parallel magnetic field,  $b = 0$  and  $b = 3$ , and for the limit  $b \rightarrow \infty$ . Panel (b) shows  $\delta G$  for  $a_\perp = 3$ ,  $b = b_\perp = 0$ , and three values of the spin-orbit parameter  $a$ :  $a = 0$ ,  $a = 0.5$  and  $a \rightarrow \infty$ . Panel (c) shows  $\delta G$  in the crossover regime, with  $a_\perp = 3.0$ ,  $a = 0.5$ , and for the same values of the parallel magnetic field as in (a). In all three plots, we have set  $b_\perp = 0$ . Choosing  $b_\perp \ll b^2$  is appropriate for small quantum dots with  $L \ll \lambda_{1,2}$ . A small nonzero value of  $b_\perp$  has only a slight effect on the shape of the curves, its general effect being to further reduce weak antilocalization.

$$\begin{aligned} C^{-1} &= N\mathbb{1} \otimes \mathbb{1} + \frac{2\pi i(\varepsilon - \varepsilon')}{\Delta} \mathbb{1} \otimes \mathbb{1} \\ &+ \frac{1}{2}[(x + x')\mathbb{1} \otimes \mathbb{1} + a_\perp(\sigma_3 \otimes \mathbb{1} - \mathbb{1} \otimes \sigma_3)]^2 \\ &+ \frac{1}{2}a^2(\sigma_1 \otimes \mathbb{1} - \mathbb{1} \otimes \sigma_1)^2 \\ &+ \frac{1}{2}a^2(\sigma_2 \otimes \mathbb{1} - \mathbb{1} \otimes \sigma_2)^2 \\ &+ i\mathbf{b} \cdot (\boldsymbol{\sigma} \otimes \mathbb{1} + \mathbb{1} \otimes \boldsymbol{\sigma}) \\ &+ \frac{1}{2}(h\sigma_3 \otimes \mathbb{1} + h'\mathbb{1} \otimes \sigma_3)^2. \end{aligned} \quad (21)$$

Setting  $x' = x$ ,  $\mathbf{b} = \mathbf{b}' = b\mathbf{e}_1$  and  $b'_\perp = b_\perp$ , we find the

average conductance,

$$\langle G \rangle = \frac{2e^2}{h} \frac{N_1 N_2}{N_1 + N_2} + \delta G, \quad (22)$$

$$\begin{aligned} \delta G &= -\frac{e^2}{h} \frac{N_1 N_2}{N_1 + N_2} \sum_{\mu, \nu} (\mathcal{TCT})_{\mu\nu; \mu\nu} \\ &= -\frac{e^2}{h} \frac{N_1 N_2}{N_1 + N_2} \left( \frac{1}{4a^2 + F_C} \right. \\ &\quad \left. + \frac{4b^2 + G_C^2 + 2G_C F_C - 16a_\perp^2 x^2}{4G_C b^2 + G_C^2 F_C - 16a_\perp^2 F_C x^2} \right), \quad (23) \end{aligned}$$

where we abbreviated

$$\begin{aligned} F_C &= N + 2(x^2 + b_\perp^2) \\ G_C &= N + 2(x^2 + a^2 + a_\perp^2). \end{aligned} \quad (24)$$

The expression for the average conductance simplifies considerably when either the perpendicular magnetic field or the parallel magnetic field is zero. In the first case,  $b = b_\perp = 0$ , one finds

$$\begin{aligned} \delta G &= \frac{e^2}{h} \frac{N_1 N_2}{N_1 + N_2} \left[ \frac{1}{N + 2x^2} - \frac{1}{4a^2 + N + 2x^2} \right. \\ &\quad \left. - \sum_{\pm} \frac{1}{2a^2 + N + 2(a_\perp \pm x)^2} \right]. \quad (25) \end{aligned}$$

This simple result can be understood recalling that the spin-orbit coupling term  $a_\perp$  acts as an effective perpendicular field with opposite sign for up and down spins. When the applied perpendicular field  $x$  exactly cancels this effective field, i.e., when  $x = \pm a_\perp$ , time-reversal symmetry is “restored” for one spin direction, leading to a weak localization-like correction to the conductance centered at  $x = \pm a_\perp$ . A non-zero value of the spin-orbit coupling term  $a$  leads to a weak antilocalization peak at  $x = 0$ , while a finite parallel magnetic fields causes a weak-localization peak at zero perpendicular field, as is illustrated in Fig. 2b and a, respectively. Both a parallel magnetic field and the spin-orbit coupling term  $a$  suppress the features at  $x = \pm a_\perp$ . (The case  $a \gg a_\perp$  is applicable when the spin-orbit coupling is not uniform, as discussed in the introduction.) Figure 2c shows an example for the dependence of the conductance  $G$  on the perpendicular field in the crossover regime when all parameters ( $a_\perp$ ,  $a$ , and  $b$ ) are important.

In the special case when the perpendicular magnetic field,  $x$ , is zero, we find

$$\begin{aligned} \delta G &= -\frac{e^2}{h} \frac{N_1 N_2}{N_1 + N_2} \left[ \frac{1}{N + 2a^2 + 2a_\perp^2} \right. \\ &\quad - \frac{2a^2 + 2a_\perp^2 - b_\perp^2}{4b^2 + (N + 2b_\perp^2)(N + 2a^2 + 2a_\perp^2)} \\ &\quad \left. + \frac{1}{N + 4a^2 + 2b_\perp^2} \right]. \quad (26) \end{aligned}$$

In the case of uniform spin-orbit scattering, this may be further simplified using  $a^2 \ll a_\perp^2$  and  $b_\perp^2 \ll b^2$ ,<sup>7</sup>

$$\begin{aligned} \delta G &= -\frac{e^2}{h} \frac{N_1 N_2}{N_1 + N_2} \left[ \frac{1}{2a_\perp^2 + N} \right. \\ &\quad \left. - \frac{1}{4a^2 + 2b_\perp^2 + N} + \frac{a_\perp^2}{4b^2 + N^2 + 2Na_\perp^2} \right]. \quad (27) \end{aligned}$$

At finite temperatures, dephasing will lead to a further suppression of weak localization. Dephasing can be included in the theory presented here by the introduction of a fictitious voltage probe.<sup>22,23,24</sup> This amounts to the replacement  $N \rightarrow N + \hbar/\tau_\phi \Delta$  in the final results (23)–(27), where  $\tau_\phi$  is the dephasing time and  $\Delta$  is the mean level spacing in the closed quantum dot.<sup>16</sup>

#### IV. CONDUCTANCE FLUCTUATIONS

Conductance fluctuations are described by the covariance of the conductance at two different values  $\varepsilon$  and  $\varepsilon'$  of the Fermi energy and at two different magnetic fields  $\mathbf{B}$  and  $\mathbf{B}'$ ,

$$\begin{aligned} \text{cov} [G(\varepsilon, \mathbf{B}), G(\varepsilon', \mathbf{B}')] &= \langle G(\varepsilon, \mathbf{B}), G(\varepsilon', \mathbf{B}') \rangle \\ &\quad - \langle G(\varepsilon, \mathbf{B}) \rangle \langle G(\varepsilon', \mathbf{B}') \rangle. \quad (28) \end{aligned}$$

For this calculation, we need to know the average of a product of four scattering matrix elements. However, if the conductance is expressed in terms of the scattering matrix  $S$  using Eq. (10), to leading order in  $1/N$ , the scattering matrix elements may be considered Gaussian random numbers, and the average of four scattering matrix elements can be factorized into products of pair averages of the form of Eq. (12).<sup>25</sup> One thus obtains

$$\begin{aligned} \text{cov} [G(\varepsilon, \mathbf{B}), G(\varepsilon', \mathbf{B}')] &= \left( \frac{e^2}{h} \right)^2 \left( \frac{N_1 N_2}{N_1 + N_2} \right)^2 \\ &\quad \times (V_D + V_C), \quad (29) \end{aligned}$$

where

$$V_D = \sum_{\mu, \nu, \mu', \nu' = \pm} D_{\mu\nu; \mu' \nu'} D_{\nu' \mu'; \nu \mu} \quad (30)$$

$$= \frac{\Xi_D}{|(b^2 - b'^2)^2 + 2K_D(-4a^2bb' + (b^2 + b'^2)L_D) + (L_D^2 - 4a^4)(K_D^2 - 4a_{\perp}^2(x - x')^2)|^2},$$

$$V_C = \sum_{\mu, \nu, \mu', \nu' = \pm} (\mathcal{TCT})_{\mu\nu; \mu' \nu'} (\mathcal{TCT})_{\mu' \nu'; \mu\nu} \quad (31)$$

$$= \frac{\Xi_C}{|(b^2 - b'^2)^2 + 2K_C(4a^2bb' + (b^2 + b'^2)L_C) + (L_C^2 - 4a^4)(K_C^2 - 4a_{\perp}^2(x + x')^2)|^2},$$

Here we abbreviated

$$\begin{aligned} \Xi_D &= 2|K_D(4a^4 - L_D^2) + 4a^2bb' - L_D(b^2 + b'^2)|^2 + 2|K_D(b^2 + b'^2) + K_D^2L_D - 4a_{\perp}^2L_D(x - x')^2|^2 \\ &\quad + 8a_{\perp}^2(x - x')^2 \left( (b + b')^2 + |L_D + 2a^2|^2 \right) \left( (b - b')^2 + |L_D - 2a^2|^2 \right) + 8|K_Dbb' + a^2(K_D^2 - 4a_{\perp}^2(x - x')^2)|^2 \\ &\quad + 4|b(b^2 - b'^2) - K_D(2a^2b' - bL_D)|^2 + 4|b'(b'^2 - b^2) - K_D(2a^2b - b'L_D)|^2 + 8|a^2(b^2 + b'^2) - bb'L_D|^2 \\ \Xi_C &= 2|K_C(4a^4 - L_C^2) - 4a^2bb' - L_C(b^2 + b'^2)|^2 + 2|K_C(b^2 + b'^2) + K_C^2L_C - 4a_{\perp}^2L_C(x + x')^2|^2 \\ &\quad + 8a_{\perp}^2(x + x')^2 \left( (b - b')^2 + |L_C + 2a^2|^2 \right) \left( (b + b')^2 + |L_C - 2a^2|^2 \right) + 8|K_Cbb' + a^2(-K_C^2 + 4a_{\perp}^2(x + x')^2)|^2 \\ &\quad + 4|b(b^2 - b'^2) + K_C(2a^2b' + bL_C)|^2 + 4|b'(b'^2 - b^2) + K_C(2a^2b + b'L_C)|^2 + 8|a^2(b^2 + b'^2) + bb'L_C|^2 \end{aligned}$$

and

$$\begin{aligned} K_D &= N + \frac{2\pi i(\varepsilon - \varepsilon')}{\Delta} + \frac{1}{2}(x - x')^2 + 2(a^2 + a_{\perp}^2) + \frac{1}{2}(b_{\perp} + b'_{\perp})^2, \\ L_D &= N + \frac{2\pi i(\varepsilon - \varepsilon')}{\Delta} + \frac{1}{2}(x - x')^2 + 2a^2 + \frac{1}{2}(b_{\perp} - b'_{\perp})^2, \\ K_C &= N + \frac{2\pi i(\varepsilon - \varepsilon')}{\Delta} + \frac{1}{2}(x + x')^2 + 2(a^2 + a_{\perp}^2) + \frac{1}{2}(b_{\perp} - b'_{\perp})^2, \\ L_C &= N + \frac{2\pi i(\varepsilon - \varepsilon')}{\Delta} + \frac{1}{2}(x + x')^2 + 2a^2 + \frac{1}{2}(b_{\perp} + b'_{\perp})^2. \end{aligned}$$

### A. Variance

The variance of the conductance at zero temperature is obtained from Eq. (29) by setting  $\varepsilon' = \varepsilon$  and  $\mathbf{B}' = \mathbf{B}$ ,

$$\begin{aligned} \text{var } G &= \frac{e^4}{h^2} \frac{N_1^2 N_2^2}{(N_1 + N_2)^2} \left[ \frac{1}{N^2} + \frac{1}{G_D^2} + \frac{8b^2 + G_D^2 + (4a^2 + N)^2}{(4a^2 G_D + 4b^2 + G_D N)^2} + \frac{1}{(4a^2 + F_C)^2} \right. \\ &\quad \left. + \frac{2F_C}{G_C(4b^2 + G_C F_C) - 16a_{\perp}^2 F_C x^2} + \frac{(4b^2 + G_C^2 + 16a_{\perp}^2 x^2)^2 + 64a_{\perp}^2 x^2 (F_C^2 - G_C^2)}{(G_C(4b^2 + G_C F_C) - 16a_{\perp}^2 F_C x^2)^2} \right]. \quad (32) \end{aligned}$$

where  $F_C$  and  $G_C$  are given by Eq. (24), and

$$G_D = N + 2(a^2 + a_{\perp}^2 + b_{\perp}^2). \quad (33)$$

Simplifications occur in the limits of zero parallel or perpendicular field, and for large perpendicular field. In the absence of a parallel field,  $b = b_{\perp} = 0$ , one finds the variance

$$\begin{aligned} \text{var } G &= \frac{e^4}{h^2} \frac{N_1^2 N_2^2}{(N_1 + N_2)^2} \left[ \frac{1}{(2a^2 + N + 2(a_{\perp} - x)^2)^2} + \frac{1}{(N + 2x^2)^2} + \frac{1}{(4a^2 + N + 2x^2)^2} \right. \\ &\quad \left. + \frac{1}{(2a^2 + N + 2(a_{\perp} + x)^2)^2} + \frac{1}{N^2} + \frac{1}{(4a^2 + N)^2} + \frac{2}{(2(a^2 + a_{\perp}^2) + N)^2} \right], \quad (34) \end{aligned}$$

while in the absence of a perpendicular magnetic field,  $x = 0$ , one has

$$\text{var } G = \frac{e^4}{h^2} \frac{N_1^2 N_2^2}{(N_1 + N_2)^2} \left[ \frac{1}{N^2} + \frac{1}{(4a^2 + 2b_\perp^2 + N)^2} + \frac{2}{[2(a^2 + a_\perp^2 + b_\perp^2) + N]^2} + \frac{2}{4b^2 + (4a^2 + N)[2(a^2 + a_\perp^2) + N]} \right. \\ \left. + \frac{2}{4b^2 + N(2(a^2 + a_\perp^2) + N)} + \frac{4(a^2 + a_\perp^2)^2}{(4b^2 + N[2(a^2 + a_\perp^2) + N])^2} + \frac{4(a^2 - a_\perp^2)^2}{(4b^2 + (4a^2 + N)[2(a^2 + a_\perp^2) + N])^2} \right]. \quad (35)$$

In the last equality we also used  $b_\perp \ll b^2$ . In the limit of large perpendicular field,  $x \gg 1$ , one has

$$\text{var } G = \frac{e^4}{h^2} \frac{N_1^2 N_2^2}{(N_1 + N_2)^2} \left[ \frac{1}{N^2} + \frac{2}{4b^2 + (4a^2 + N)[2(a^2 + a_\perp^2 + b_\perp^2) + N]} \right. \\ \left. + \frac{1}{[2(a^2 + a_\perp^2 + b_\perp^2) + N]^2} + \frac{4(-a^2 + a_\perp^2 + b_\perp^2)^2}{(4b^2 + (4a^2 + N)[2(a^2 + a_\perp^2 + b_\perp^2) + N])^2} \right]. \quad (36)$$

When both the perpendicular and the parallel field are large, i.e.  $x^2, b \gg a_\perp^2, a^2, b_\perp^2, N$  a particularly simple expression for the variance results

$$\text{var } G = \frac{e^4}{h^2} \frac{N_1^2 N_2^2}{(N_1 + N_2)^2} \left[ \frac{1}{N^2} + \frac{1}{(N + 2a^2 + 2a_\perp^2 + 2b_\perp^2)^2} \right].$$

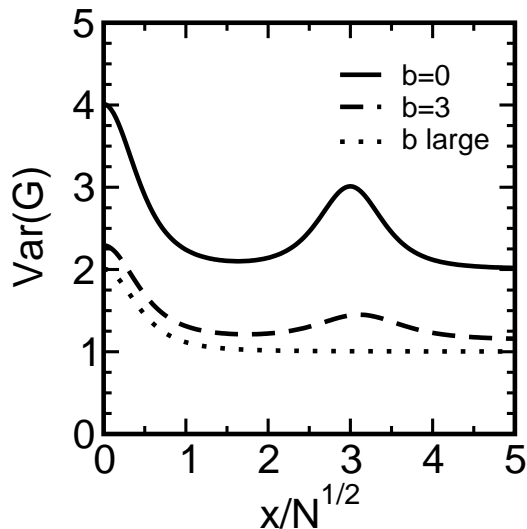


FIG. 3: Conductance fluctuations  $\text{var } G$ , measured in units of  $[(e^2/h)(N_1 N_2)/(N_1 + N_2)^2]^2$  as a function of the perpendicular magnetic field  $x$ , for  $a_\perp = 3$ ,  $a = 0$ ,  $b_\perp = 0$ . From bottom to top, the curves are for  $b = 0$ ,  $b = 3$ , and for the limit  $b \rightarrow \infty$ .

The variance of the conductance in the presence of spin-orbit coupling is shown in Fig. 3, for three different parallel field strengths. An increase of the conductance fluctuations is observed around  $x = \pm a_\perp$ . This feature is explained noting that at  $x = \pm a_\perp$  the perpendicular magnetic field exactly cancels the effective magnetic field due to the spin-orbit coupling term  $a_\perp$  for one spin direction, so that the effective Hamiltonian for that spin

direction is real, not complex. A parallel field and the spin-orbit coupling term  $a$  suppress this feature (data for  $a$  not shown). Both effects also reduce the variance at zero perpendicular field by a factor of two.

At finite temperatures, both the effects of thermal smearing and dephasing need to be taken into account for a calculation of the variance of the conductance. Dephasing (with dephasing time  $\tau_\phi$ ) is incorporated in the results (29)–(37) by the substitution  $N \rightarrow N + \hbar/\tau_\phi\Delta$ . The effect of thermal smearing requires an integration over the energies  $\varepsilon$  and  $\varepsilon'$ ,

$$\text{var } G(T) = \int d\varepsilon d\varepsilon' \frac{df}{d\varepsilon} \frac{df}{d\varepsilon'} \text{cov}[G(\varepsilon), G(\varepsilon')], \quad (37)$$

where  $f$  is the Fermi distribution function. The integrations over energy needs to be done by numerical methods in all but a few special cases. We refer to Ref. 26 for details. Equation (37) was used for a quantitative comparison of theory and experiment by Zumbühl *et al.*<sup>15</sup>

### B. Symmetry with respect to perpendicular magnetic field inversion

The presence of spin-orbit coupling has interesting consequences for the symmetry of the conductance under reversal of the perpendicular field. Although, in general, the conductance does not change when the total magnetic field is reversed,  $b \rightarrow -b$ ,  $b_\perp \rightarrow -b_\perp$ , and  $x \rightarrow -x$ , the conductance need not be symmetric under reversal of the perpendicular component  $x$  only. In order to study the symmetry of the conductance under reversal of the perpendicular component  $x$  of the magnetic field, we con-



sider the correlator

$$Q(x) = \frac{\langle G(x)G(-x) \rangle - \langle G(x) \rangle^2}{\text{var } G(x)} \quad (38)$$

for  $x^2 \gg N$ . Perfect symmetry under reversal of the perpendicular component of the magnetic field only implies  $Q(x) = 1$ , while the absence of any correlations between  $G(x)$  and  $G(-x)$  implies  $Q(x) = 0$ .

Note that the invariance of the two-terminal conductance under a complete reversal of the magnetic field implies that

$$\langle G(x, b)G(-x, b) \rangle = \langle G(x, b)G(x, -b) \rangle,$$

so that  $Q$  can also be defined as a correlator for conductances at opposite values of the parallel magnetic field, keeping the perpendicular field constant.

In the absence of an in-plane magnetic field, reversal of the perpendicular magnetic field component is the same as reversal of the total magnetic field, so that  $G$  is trivially symmetric in  $x$ . In the absence of spin-orbit scattering, the sole effect of the parallel magnetic field is to lift spin degeneracy, and symmetry of  $G$  follows from the fact that the conductance for each spin species is symmetric in  $x$ . In the presence of both spin-orbit scattering and an in-plane field, there is no general symmetry that requires that  $G$  is symmetric under reversal  $B_3 \rightarrow -B_3$ , however the measure of observable asymmetry depends upon to what cross-over symmetry class the generated random matrix theory ensemble belongs.

Indeed, calculation of the correlator  $Q(x)$  using our general result (29) for the covariance of the conductance shows that the symmetry of the conductance with respect to reversal of the perpendicular component of the magnetic field is destroyed when either  $b \neq 0$  and  $a \neq 0$ ,  $b_\perp \neq 0$  and  $a_\perp \neq 0$ , or  $b_\perp \neq 0$  and  $a \neq 0$ . In the case  $a = 0$  and  $b_\perp = 0$ , the conductance remains symmetric in  $x$ , even if  $a_\perp \neq 0$  and  $b \neq 0$ . In that case, the effective Hamiltonian (4) still has the extra symmetry  $\sigma_1 \tilde{\mathcal{H}} \sigma_1 = \tilde{\mathcal{H}}$ , which ensures the symmetry with respect to the perpendicular magnetic field reversal.<sup>7</sup> Symmetry in the perpendicular component of the magnetic field is also preserved if the parallel magnetic field is so large that both  $b, b_\perp \neq 0$ , but  $a_\perp^2 \ll N$  and  $a^2 \ll N$ , see Ref. 7 for a symmetry argument. Figure 4 shows plots of  $Q(x)$  for the two minimal cases  $a = 0$  or  $b_\perp = 0$ .

The general parameter dependence of  $Q(x)$  for  $x^2 \gg N$  can be obtained from Eq. (29). Simple expressions are found in the cases  $b \gg N$  and  $a_\perp^2 \gg N$ , for which we have

$$Q = \frac{N^2}{(4a^2 + 2b_\perp^2 + N)^2}, \quad (39)$$

and for  $b \gg N$ , while still  $b_\perp = 0$ ,

$$Q = 1 - \left[ 1 - \frac{N^2}{(4a^2 + N)^2} \right] \times \left[ 1 - \frac{N^2}{2[(a^2 + a_\perp^2)^2 + (a^2 + a_\perp^2 + N)^2]} \right]. \quad (40)$$

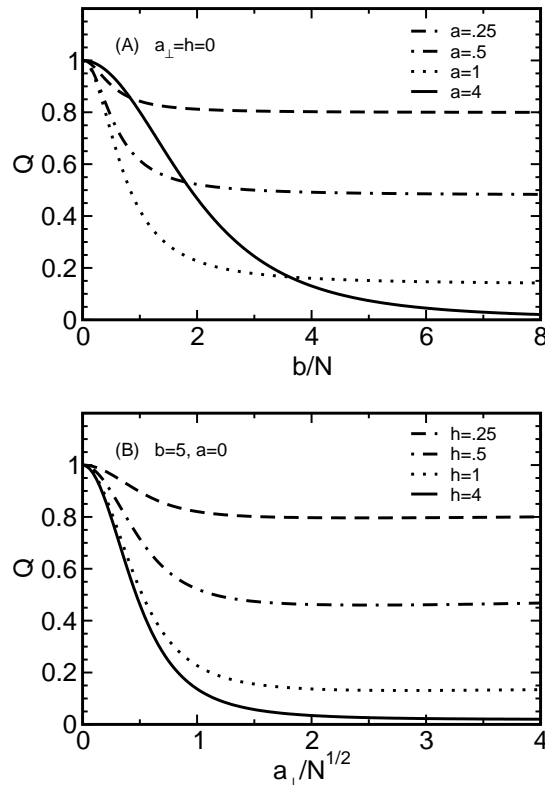


FIG. 4: The correlator  $Q(x) = (\langle G(x)G(-x) \rangle - \langle G(x) \rangle^2) / \text{var } G(x)$  for  $x^2 \gg N$ . In panel (a),  $Q$  is shown as a function of parallel field  $b$ , with  $a_\perp = b_\perp = 0$ . In panel (b),  $Q$  is shown as a function of spin-orbit coupling  $a_\perp$ , with  $b = 5$  and  $a = 0$ .

On the other hand, if  $b \gg N$  and  $b_\perp \gg N$ , the correlation function  $Q$  is given by

$$Q = \frac{N^2}{(2a^2 + 2a_\perp^2 + N)^2}, \quad (41)$$

confirming that  $G$  remains a symmetric function of  $x$  if  $b$  and  $b_\perp$  are large but  $a$  and  $a_\perp$  are not.

Experimentally, the component of the conductance fluctuations that is antisymmetric with respect to the reversal  $B_3 \rightarrow -B_3$  in the presence of in-plane magnetic field can be used as a test to the strength of spin-orbit coupling, even if  $b \ll N$ . This is because an alternative mechanism of time-reversal symmetry breaking by an in-plane magnetic field via the inter-subband mixing<sup>17</sup> generates anti-symmetric conductance fluctuations in the third order in the field only, thus  $1 - Q(x \gg N) \sim B_\parallel^6$ . In contrast, the spin-orbit-coupling induced asymmetry, which can be analyzed by expanding  $Q(x)$  with respect to  $b^2$  and  $b_\perp^2$ , has

$$\begin{aligned}
Q = & 1 - 4[4a^2b^2(32a^4a_\perp^4 + 24a^2a_\perp^4N + 6a_\perp^4N^2 + 4a_\perp^2N^3 + N^4) \\
& + a_\perp^2b_\perp^2(128a^6a_\perp^4 + 96a^4a_\perp^4N + 24a^2a_\perp^4N^2 + 4a_\perp^4N^3 + 6a_\perp^2N^4 + 3N^5)] \\
& \times [N(4a^2 + N)(2a_\perp^2 + N)(16a^4a_\perp^4 + 8a^2a_\perp^4N + 2a_\perp^4N^2 + 2a_\perp^2N^3 + N^4)]^{-1},
\end{aligned} \tag{42}$$

for the case of uniform spin-orbit coupling. In the limit of a dot with a large number of channels  $N \gg a_\perp^2$  but still in the universal regime  $N \ll E_{\text{Th}}/\Delta$ , this simplifies to

$$Q = 1 - 16a^2b^2N^{-3}. \tag{43}$$

Replacing the dimensionless spin-orbit coupling and magnetic field  $a_\perp$  and  $b_\perp$  by their dimensionful counterparts, one arrives at the result (9) advertised in the introduction.

### C. Autocorrelation function and the “correlation echo”

Correlations between the conductance  $G$  at different values of the perpendicular magnetic field  $x$  are studied through the conductance autocorrelation function

$$\chi(x, x') = \langle G(x)G(x') \rangle - \langle G(x) \rangle \langle G(x') \rangle. \tag{44}$$

For large perpendicular fields,  $x^2, x'^2 \gg N$ , the autocorrelator  $\chi(x, x')$  depends on the difference  $(x - x')$  only. Since time-reversal symmetry is fully broken for such large magnetic fields, any features in the autocorrelator are signatures of the spin-orbit coupling.

For zero parallel field,  $b = b_\perp = 0$ , one finds from Eq. (29),

$$\begin{aligned}
\chi(\xi) = & \left( \frac{2e^2}{h} \frac{N_1 N_2}{N_1 + N_2} \right)^2 \left[ \frac{1}{(2N + 8a^2 + \xi^2)^2} \right. \\
& + \frac{1}{(2N + \xi^2)^2} + \frac{1}{(2N + 4a^2 + (-2a_\perp + \xi)^2)^2} \\
& \left. + \frac{1}{(2N + 4a^2 + (2a_\perp + \xi)^2)^2} \right],
\end{aligned} \tag{45}$$

where  $\xi = x - x'$ .

A plot of  $\chi(x - x')$  for different values of  $a_\perp$  is shown in Fig. 5. Remarkably, the conductance autocorrelator shows an “echo” at  $|x - x'| = 2a_\perp$ . This echo appears even for large values of  $a_\perp$ , for which the conductance correlations have decayed for intermediate values of the magnetic-field difference, see Fig. 5a. The magnetic-field echo has the same origin as the reappearance of the weak localization and conductance fluctuations at finite values of the perpendicular magnetic field  $x$ : The spin-orbit term  $a_\perp$  acts as a homogeneous perpendicular field with a different direction for the up and down spins (defined with respect to the axis  $\hat{\mathbf{e}}_3$  perpendicular to the plane of

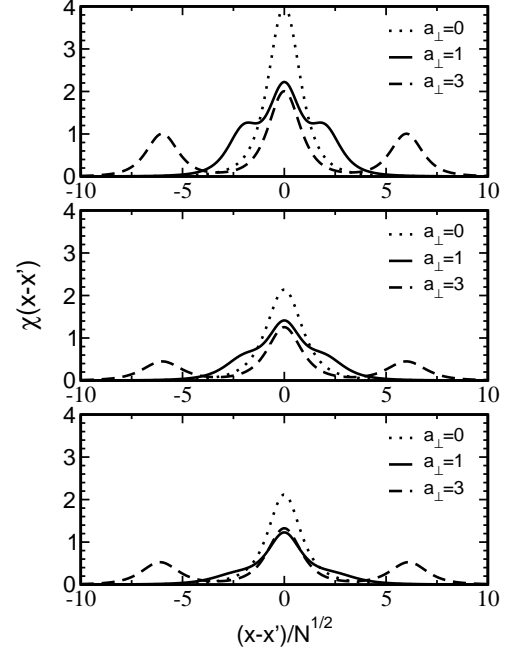


FIG. 5: The correlator  $\chi(x - x')$  as a function of the dimensionless perpendicular magnetic field difference  $(x - x')$ , for three values of the spin-orbit term  $a_\perp$ :  $a_\perp = 0$ ,  $a_\perp = 1$ , and  $a_\perp = 3$ . Curves in panel (a) are for  $a = 0$  and  $b = b_\perp = 0$ . Curves in panel (b) are for  $a = 0.5$  and  $b = b_\perp = 0$ . Panel (c) shows the effect of the parallel field,  $b = 2$ , with  $a = b_\perp = 0$ . In all three panels,  $\chi(x - x')$  is measured in units of  $[(e^2/h)N_1^2N_2^2/(N_1 + N_2)^2]^2$ .

the quantum well). In the presence of an external perpendicular magnetic field  $x$ , Up spins and down spins experience effective perpendicular magnetic fields  $x + a_\perp$  and  $x - a_\perp$ , respectively. If the magnetic field difference  $x - x'$  equals  $\pm 2a_\perp$ , one spin species at field  $x$  moves in the same effective perpendicular field as the other spin species at field  $x'$ . Hence, in the absence of a parallel field and a spin-orbit term  $a$ , the conductance has identical fluctuating contributions at  $x$  and  $x'$ . However, only one spin species is involved in the “echo” — the autocorrelation function reaches only one half of the total variance of the conductance; the other spin species have uncorrelated contributions to the conductance at the external fields  $x$  and  $x'$ . A magnetic field in the plane of the quantum well and the spin-orbit coupling term  $a$  suppress the echo, since they cause scattering between the  $\pm\hat{\mathbf{e}}_3$  spin

directions, see Figs. 5b and c.

## V. EFFECT OF A NON-UNIFORM SO COUPLING.

The expressions of the previous two sections are valid for arbitrary magnitudes of the dimensionless spin-orbit rates  $a_{\perp}$  and  $a$ . In the case of uniform spin-orbit coupling, one has the strong inequality  $a \ll a_{\perp}$ . In general, the spin-orbit coupling may be non-uniform throughout the quantum dot, *e.g.*, as a result of a spatial modulation of the asymmetry of the quantum well or as a result of a modulation of the electron density (and therefore confining potential width) across the dot. The main effect of a non-uniformity of the spin-orbit coupling is an increase of  $a$ ,<sup>16</sup> thus promoting the crossover into the standard symplectic ensemble. In this section, we'll give a quantitative estimate of this effect for a special choice of the non-uniformity. Another effect of a non-uniform spin-orbit coupling is a rescaling of  $a_{\perp}$ , and will not be considered here.

Assuming that the non-uniformity of spin-orbit coupling affects only its strength without changing the generic form of the Hamiltonian, we describe its effect via coordinate dependent spin-orbit coupling lengths  $\lambda_{1,2}^{-1}(\mathbf{r})$ ,

$$\begin{aligned} \mathcal{H} &= \frac{1}{2m} (\mathbf{p} - e\mathbf{A} - \mathbf{a})^2, \\ \mathbf{a} &= \frac{\sigma_2}{2\lambda_1(\mathbf{r})} \hat{\mathbf{e}}_1 - \frac{\sigma_1}{2\lambda_2(\mathbf{r})} \hat{\mathbf{e}}_2. \end{aligned} \quad (46)$$

In the case that

$$\beta = \nabla \times \mathbf{a} = \frac{\sigma_2}{2} \partial_{x_2} \lambda_1^{-1}(\mathbf{r}) + \frac{\sigma_1}{2} \partial_{x_1} \lambda_2^{-1}(\mathbf{r}) \neq 0,$$

it is not possible to eliminate the spin-orbit coupling from the Hamiltonian in the first order in spin-orbit coupling constant by a unitary transformation. Qualitatively, this explains why the spatial variation of the spin-orbit coupling length gives rise of a term with the symmetry of  $\mathbf{a}_{\parallel}$ . For a quantitative estimate of how much the spatial variations of  $\lambda_{1,2}$  contribute to the energy scale  $\varepsilon_{\parallel}$ , we note that it is still possible to find a transformation  $U$  such that the resulting non-Abelian vector potential in a locally rotated spin frame,

$$\tilde{\mathbf{a}} = -iU^{\dagger} \nabla U - U^{\dagger} \mathbf{a} U, \quad (47)$$

would satisfy the conditions

$$\nabla \cdot \tilde{\mathbf{a}} = 0 \quad (48)$$

in the interior of the quantum dot and  $\hat{\mathbf{n}} \cdot \tilde{\mathbf{a}} = 0$ , on the dot boundary, where  $\hat{\mathbf{n}}$  is the unit vector normal to the dot's boundary, at least, in the lowest order in SO coupling. Such conditions would enable one to satisfy boundary conditions for Cooperon and diffuson propagators from diagrammatic perturbation theory, which is

needed in order to make the zero-dimensional approximation necessary for the use of random matrix theory. This program is carried out in the appendix for a circular quantum dot with a special choice of the coordinate dependence of the spin-orbit coupling lengths  $\lambda_{1,2}$ .

Here, as an example, we consider here the case where the spin-orbit coupling is stronger in the center of a quantum dot (where density is higher and the well is narrower) than at the edges (where density is lower and the well is broader),

$$\frac{1}{\lambda_{1,2}} = \frac{1}{\lambda^c} - \frac{(r/L)^2}{\lambda^f}, \quad (49)$$

where  $L$  is the typical size of the dot, without making a restriction of the size of the dot. We perform a unitary transformation

$$U = \exp \left( i \frac{x_1 \sigma_2 - x_2 \sigma_1}{2\lambda^c} \left[ 1 - \frac{\lambda^c}{3\lambda^f} \left( \frac{r}{L} \right)^2 \right] \right), \quad (50)$$

which rotates to a local spin reference axis. With this transformation, the matrix vector  $\tilde{\mathbf{a}}$  becomes, to lowest order in the inverse spin-orbit coupling length,

$$\begin{aligned} \tilde{\mathbf{a}} &= -iU^{\dagger} \nabla U - \mathbf{a} + \mathcal{O}(\lambda^{-2}) \\ &= -\frac{x_1 \sigma_1 + x_2 \sigma_2}{3\lambda^f L^2} [\hat{\mathbf{e}}_3 \times \mathbf{r}]. \end{aligned} \quad (51)$$

We conclude that (a) the spin relaxation and the crossover into symplectic ensemble start, indeed, in the lowest order in the non-uniform part of the spin-orbit coupling and (b) for the non-uniform coupling (49), the functional form of the perturbation after transformation is equal to that of the term  $\mathbf{a}_{\parallel}$  in Eq. (4). The latter observation allows us to express the contribution of the non-uniformity to the energy scale  $\varepsilon_{\parallel}$  as

$$\varepsilon_{\parallel} = \frac{1}{4} \kappa' \kappa E_{\text{Th}} \left( \frac{L^2}{4\lambda^f{}^2} \right), \quad (52)$$

where the geometry-dependent coefficients  $\kappa$  and  $\kappa'$  are the same as those defined for the spatially homogeneous spin-orbit coupling in Eq. (6).

## VI. CONCLUSIONS

In this paper we calculated the average and the fluctuations of the conductance of a chaotic quantum dot in the presence of Bychkov-Rashba and (linear) Dresselhaus spin-orbit coupling and a magnetic field and studied the symmetry of the conductance under reversal of the perpendicular component of the magnetic field. The calculations were done to leading order in  $1/N$ , where  $N = N_1 + N_2$  is the total number of open channels in the leads connecting the quantum dot to the reservoirs. After a unitary transformation, the spin-orbit term in the Hamiltonian and the Zeeman coupling to the external magnetic field are transformed into four terms that

all have different symmetries.<sup>7</sup> The corresponding energy scales are the conventional Zeeman energy  $\varepsilon^Z = \mu_B g B$  and three energy scales that depend on the spin-orbit coupling: two spin-orbit scales  $\varepsilon_{\perp}^{\text{so}}$  and  $\varepsilon_{\parallel}^{\text{so}}$ , and the second Zeeman energy scale  $\varepsilon_{\perp}^Z$ . With the help of the theory presented here, the energy scales  $\varepsilon_{\perp}^{\text{so}}$ ,  $\varepsilon_{\parallel}^{\text{so}}$ , and  $\varepsilon_{\perp}^Z$  can be obtained from a measurement of the conductance auto-correlation function of the quantum dot.

Our results provide several routes to a direct measurement of the product of the spin-orbit coupling lengths  $\lambda_1$  and  $\lambda_2$ . The product  $\lambda_1 \lambda_2$  can be found from a “magnetic-field echo” in the conductance fluctuations as a function of the perpendicular magnetic field. The magnetic-field echo appears at the magnetic-field difference

$$\Delta B = \frac{\hbar}{e \lambda_1 \lambda_2}. \quad (53)$$

The same magnetic-field scale splits the weak-localization peak in the absence of a parallel magnetic field. The ratio  $\lambda_1/\lambda_2$  can be found from a measurement of the energy scale  $\varepsilon_{\perp}^Z$  in a roughly circular quantum dot. In this case,  $(\lambda_2/\lambda_1)^2$  is equal to the ratio of the energy scales  $\varepsilon_{\perp}^Z$  for the in-plane magnetic field in the crystallographic directions  $\hat{e}_1 = [110]$  and  $\hat{e}_2 = [1\bar{1}0]$ . Measurement of  $\varepsilon_{\parallel}^{\text{so}}$  is less suitable to determine  $\lambda_1/\lambda_2$ , as it may be affected by non-uniformities in the spin-orbit scattering rate.

The theory presented here has been used for the interpretation of measurements of the conductance of quantum dots in GaAs/GaAlAs heterostructures with spin-orbit coupling as a function of parallel and perpendicular components of the magnetic field by Zumbühl *et al.*<sup>15</sup> The quantum dots used in the experiments of Ref. 15 were built of the same material, but they varied in size, ranging from  $L/\lambda = 0.27$  to 0.64. Here  $\lambda = (\lambda_1 \lambda_2)^{1/2}$  is the geometric average of the spin-orbit lengths  $\lambda_1$  and  $\lambda_2$ . Whereas the conductance of smaller dots had a minimum at zero perpendicular magnetic field, the conductance of larger dots had a (local) maximum at zero magnetic field. From a fit to our expression for the average conductance at zero parallel field, Eq. (23), values for the experimentally unknown parameters  $\lambda = 4.4 \mu\text{m}$ , the decoherence time  $\tau_{\phi}$  and a geometrical factor, see Eqs. (6), were extracted. Measurement of the average conductance in the presence of a magnetic field parallel to the plane of the two-dimensional electron gas was in good agreement with our Eq. (23), without additional fit parameters and up to a parallel field of about 0.3 T.<sup>15</sup> Upon inclusion of the effects of time-reversal symmetry breaking by a strong parallel field due to the finite extent of the electron wavefunction across the heterostructure,<sup>17</sup> the authors of Ref. 15 could extend the agreement between theory and experiment is extended to even higher magnetic fields.

## Acknowledgments

We thank Igor Aleiner, Boris Altshuler, Bertrand Halperin, Charles Marcus, Jeffrey Miller, Yuli Nazarov, and Dominik Zumbühl for important discussions. This work was supported by NSF under grant no. PHY 0117795 (JC), by the NSF under grant no. DMR 0086509 and by the Packard foundation (PWB), and by EPSRC and NATO CLG (VF).

## APPENDIX A: GEOMETRY-DEPENDENT COEFFICIENTS FOR A CIRCULAR QUANTUM DOT

In this appendix, we calculate

$$\mathcal{D}_{\mu_1 \nu_1; \mu_2 \nu_2}(\mathbf{r}_1, \mathbf{r}_2) = \langle G_{\mu_1 \nu_1}^{\text{R}}(\mathbf{r}_1, \mathbf{r}_2)(E, B) \times G_{\mu_2 \nu_2}^{\text{A}}(\mathbf{r}_1, \mathbf{r}_2)(E', B') \rangle \quad (\text{A1})$$

for a disordered circular quantum dot with spin-orbit scattering. Here  $G^{\text{R}}$  and  $G^{\text{A}}$  are the retarded and advanced Green functions (inverses of  $\varepsilon - \mathcal{H}$  for  $\varepsilon$  just above and just below the real axis, respectively), respectively, and the indices  $\mu_1$ ,  $\mu_2$ ,  $\nu_1$ , and  $\nu_2$  refer to the electron spin. Comparison of our result with the random matrix theory of Sec. III allows us to find the geometry-dependent coefficients  $\kappa$ ,  $\kappa'$ , and  $\kappa''$  of Eqs. (6).

In a closed dot of volume  $V$  and with diffusive dynamics, the diffuson  $\mathcal{D}(\mathbf{r}_1, \mathbf{r}_2)$  obeys the equation

$$(i\hbar\omega + \Pi)\mathcal{D}(\mathbf{r}_1, \mathbf{r}_2) = \frac{2\pi}{V\Delta} \delta(\mathbf{r}_1 - \mathbf{r}_2) \mathbb{1} \otimes \mathbb{1}, \quad (\text{A2})$$

where  $\hbar\omega = \varepsilon' - \varepsilon$  and the differential operator  $\Pi$  is given by

$$\Pi = (D/\hbar)(-i\hbar\nabla_{\mathbf{r}_1} + \mathbf{a} \otimes \mathbb{1} - \mathbb{1} \otimes \mathbf{a}')^2 + ih_Z \otimes \mathbb{1} - i\mathbb{1} \otimes h'_Z. \quad (\text{A3})$$

Here  $D = v_F l/2$  is the diffusion coefficient in the quantum dot, the matrix vector potentials  $\mathbf{a}$  and  $\mathbf{a}'$  are the sum of a spin-independent contribution from the perpendicular magnetic field and a spin-dependent contribution from the Bychkov-Rashba and Dresselhaus spin-orbit coupling,

$$\begin{aligned} \mathbf{a} &= \left( \frac{eB_3 y}{2c} - \frac{\hbar}{2\lambda_1} \sigma_2 \right) \hat{e}_1 - \left( \frac{eB_3 x}{2c} - \frac{\hbar}{2\lambda_2} \sigma_1 \right) \hat{e}_2, \\ \mathbf{a}' &= \left( \frac{eB'_3 y}{2c} - \frac{\hbar}{2\lambda_1} \sigma_2 \right) \hat{e}_1 - \left( \frac{eB'_3 x}{2c} - \frac{\hbar}{2\lambda_2} \sigma_1 \right) \hat{e}_2, \end{aligned} \quad (\text{A4})$$

while  $h_Z$  and  $h'_Z$  represent the Zeeman coupling to the magnetic field,

$$h_Z = \frac{1}{2} \mu_B g \mathbf{B} \cdot \boldsymbol{\sigma}, \quad h'_Z = \frac{1}{2} \mu_B g \mathbf{B}' \cdot \boldsymbol{\sigma}.$$

Equation (A2) is supplemented with the boundary condition

$$\hat{n} \cdot (-i\hbar\nabla_{\mathbf{r}_1} + \mathbf{a} \otimes \mathbf{1} - \mathbf{1} \otimes \mathbf{a}')\mathcal{D}(\mathbf{r}_1, \mathbf{r}_2) = 0 \quad (\text{A5})$$

at the sample boundary, where  $\hat{n}$  is the unit vector normal to the boundary.

To find  $\mathcal{D}$ , we shift to the basis of eigenfunctions of the diffusion equation (i.e., eigenfunctions of  $\Pi$  in the absence of spin-orbit scattering and a magnetic field) and calculate the matrix elements of  $\Pi$  in that basis. For this procedure to work, it is important that the matrix vector potentials  $\mathbf{a}$  and  $\mathbf{a}'$  do not change the Von Neumann boundary conditions (A5), i.e., that

$$\hat{n} \cdot \mathbf{a} = \hat{n} \cdot \mathbf{a}' = 0 \quad (\text{A6})$$

at the boundary of the quantum dot. This requirement ensures that the eigenfunctions of the diffusion equation with Von Neumann boundary conditions can be used to construct the diffuson  $\mathcal{D}$ . In order to fix the gauge, we also require that

$$\nabla \cdot \mathbf{a} = \nabla \cdot \mathbf{a}' = 0 \quad (\text{A7})$$

in the interior of the dot (London gauge).

As discussed in Ref. 7 and in the introduction of this paper, the requirements (A6) and (A7) are realized by performing a suitable unitary transformation  $U$  to the Hamiltonian,  $\mathcal{H} \rightarrow U^\dagger \mathcal{H} U$ . For Eq. (A2), such a unitary transformation implies

$$\mathcal{D} \rightarrow (U^\dagger \otimes U)\mathcal{D}(U \otimes U^\dagger), \quad (\text{A8})$$

$$\Pi \rightarrow (U^\dagger \otimes U)\Pi(U \otimes U^\dagger). \quad (\text{A9})$$

We'll now perform an explicit calculation for the case of a circular quantum dot of radius  $L$ , the origin of our coordinate system being chosen at the center of the dot. In polar coordinates  $x_1 = r \cos \phi$ ,  $x_2 = r \sin \phi$ , the tensor eigenfunctions of the diffusion equation are of the form

$$\begin{aligned} f_{n0}^{ij}(r, \phi) &= c_{n0} J_0(rx_{n0}/L) \sigma_i \otimes \sigma_j, \\ f_{nm}^{ij}(r, \phi) &= c_{nm} J_m(rx_{nm}/L) \cos(m\phi) \sigma_i \otimes \sigma_j, \\ g_{nm}^{ij}(r, \phi) &= c_{nm} J_m(rx_{nm}/L) \sin(m\phi) \sigma_i \otimes \sigma_j \end{aligned} \quad (\text{A10})$$

where  $i, j = 0, 1, 2, 3$ ,  $m = 1, 2, \dots$ ,  $x_{nm}$ ,  $n = 1, 2, \dots$ , is the  $n$ th positive root of  $J'_m(x) = 0$ , and we used the

notation  $\sigma_0 = \mathbf{1}$ . The corresponding eigenvalues are

$$\lambda_{nm} = D\hbar(x_{nm}/L)^2 \quad (\text{A11})$$

and the normalization constants are

$$c_{nm}^{-2} = \frac{1}{2}\pi L^2 (J_m(x_{nm})^2 - J_{m+1}(x_{nm})^2)(1 + \delta_{m0}). \quad (\text{A12})$$

The smallest eigenvalue is found for  $n = m = 0$ ,  $\lambda_{00} = 0$ ; all other eigenvalues are larger than the Thouless energy  $E_{\text{Th}} = D\hbar/L^2$ .

For a circular quantum dot, the magnetic-field contribution to the matrix vector potential of Eq. (A3) already satisfies the requirements (A6) and (A7). For the spin-orbit contribution we use the transformation

$$\begin{aligned} U &= \exp \left[ i \frac{x_1 \sigma_2}{2\lambda_1} - i \frac{x_2 \sigma_1}{2\lambda_2} \right. \\ &\quad \left. - i \frac{(x_1^2 + x_2^2 - 3L^2)}{48\lambda_1\lambda_2} \left( \frac{x_2 \sigma_1}{\lambda_1} - \frac{x_1 \sigma_2}{\lambda_2} \right) \right], \end{aligned} \quad (\text{A13})$$

which fulfills the requirements (A6) and (A7) to leading order in  $L/\lambda$ . [Note: although the transformation of Eq. (2) is sufficient to satisfy the requirements to order  $L/\lambda$ , the remaining term  $a_{\parallel}$  of Eq. (4) does not obey Eq. (A7).]

With this transformation, the matrix vector potential  $\mathbf{a}$  and the Zeeman term  $h_Z$  change to

$$\begin{aligned} \mathbf{a} &\rightarrow \hat{\mathbf{e}}_1 \left[ \frac{eB_3 x_2}{2c} + \frac{\hbar x_2 \sigma_3}{4\lambda_1 \lambda_2} \right. \\ &\quad \left. + \frac{\hbar}{16\lambda_1 \lambda_2} \left( \frac{2x_1 x_2 \sigma_1}{\lambda_1} + \frac{(3x_2^2 + x_1^2 - L^2)\sigma_2}{\lambda_2} \right) \right] \\ &\quad - \hat{\mathbf{e}}_2 \left[ \frac{eB_3 x_1}{2c} + \frac{\hbar x_1 \sigma_3}{4\lambda_1 \lambda_2} \right. \\ &\quad \left. + \frac{\hbar}{16\lambda_1 \lambda_2} \left( \frac{2x_1 x_2 \sigma_2}{\lambda_2} + \frac{(3x_1^2 + x_2^2 - L^2)\sigma_1}{\lambda_1} \right) \right], \\ h_Z &\rightarrow \frac{1}{2}\mu_B g \mathbf{B} \cdot \boldsymbol{\sigma} - \frac{1}{2}\sigma_3 \mu_B g \left( \frac{B_1 x_1}{\lambda_1} + \frac{B_2 x_2}{\lambda_2} \right), \end{aligned} \quad (\text{A14})$$

with similar changes for  $\mathbf{a}'$  and  $h'_Z$ .

As long as all relevant energy scales are much smaller than  $E_{\text{Th}}$ , it is sufficient to know the action of  $\Pi$  on the 16 eigenfunctions at  $f_{00}^{ij}$  at  $n = m = 0$ . In tensor notation, this action is

$$\begin{aligned} \Pi &= \frac{D\hbar}{2L^2} \left( \frac{e}{ch} (\Phi - \Phi') \mathbf{1} \otimes \mathbf{1} + \frac{L^2}{4\lambda^2} (\sigma_3 \otimes \mathbf{1} - \mathbf{1} \otimes \sigma_3) \right)^2 \\ &\quad + \frac{D\hbar L^6}{96\lambda^4} \left( \frac{\sigma_1 \otimes \mathbf{1} - \mathbf{1} \otimes \sigma_1}{2\lambda_1} \right)^2 + \frac{D\hbar L^6}{96\lambda^4} \left( \frac{\sigma_2 \otimes \mathbf{1} - \mathbf{1} \otimes \sigma_2}{2\lambda_2} \right)^2 \\ &\quad + i \frac{\mu_B g \mathbf{B}}{2} (\boldsymbol{\sigma} \otimes \mathbf{1} - \mathbf{1} \otimes \boldsymbol{\sigma}) + \frac{\mu_B^2 g^2 L^4}{D\hbar} \kappa_h \left( \frac{B_1^2}{\lambda_1^2} + \frac{B_2^2}{\lambda_2^2} \right) (\mathbf{1} \otimes \sigma_3 - \sigma_3 \otimes \mathbf{1})^2. \end{aligned} \quad (\text{A15})$$

where  $\Phi = B_3\pi L^2$  is the magnetic flux through the quantum dot and

$$\kappa_h = \frac{1}{2} \sum_{n=1}^{\infty} \frac{1}{x_{1n}^4 (x_{1n}^2 - 1)} \approx 0.0182$$

is a numerical constant. Confining ourselves to the case  $\lambda = \lambda_1 = \lambda_2$  and comparing this result to Eq. (20), we can make the identifications

$$x^2 = \left( \frac{e\Phi}{ch} \right)^2 \frac{\hbar v_F l \pi}{L^2 \Delta}, \quad (\text{A16})$$

$$a_{\perp}^2 = \left( \frac{L^2}{4\lambda^2} \right)^2 \frac{\hbar v_F l \pi}{L^2 \Delta}, \quad (\text{A17})$$

$$a^2 = \left( \frac{L^2}{4\lambda^2} \right)^3 \frac{v_F l \pi}{3L^2 \Delta}, \quad (\text{A18})$$

$$b = \frac{\mu_B g \pi B}{\Delta}, \quad (\text{A19})$$

$$b_{\perp} \approx 1.83 \frac{L^2}{\hbar v_F l \Delta} (\mu_B B g)^2 \left( \frac{L^2}{4\lambda^2} \right). \quad (\text{A20})$$

For the geometry-dependent constants  $\kappa$ ,  $\kappa'$ , and  $\kappa''$  in Eq. (6), this implies  $\kappa = 2$ ,  $\kappa' = 1/3$  and  $\kappa'' \approx 0.292$ .

If the spin-orbit coupling is not uniform throughout the quantum dot, see Sec. V, the above estimates for  $a_{\perp}$  and  $a$  and the corresponding energy scales  $\varepsilon_{\perp}^{\text{so}}$  and  $\varepsilon_{\parallel}^{\text{so}}$  need to be revisited. Here we consider the example of Eq. (49),  $\lambda_{1,2}^{-1}(\mathbf{r}) = \lambda_c^{-1} + (r^2/L^2\lambda^f)$ , and construct the unitary transformation  $U$  that ensures that the conditions (A6) and (A7) are satisfied to lowest order in  $1/\lambda_f$ ,

$$U = \exp \left[ i \frac{x_1 \sigma_2}{2\lambda_1^c} - i \frac{x_2 \sigma_1}{2\lambda_2^c} + i x_1 \sigma_2 \frac{(x_1^2 + x_2^2 + L^2)}{8L^2 \lambda_1^f} - i x_2 \sigma_1 \frac{(x_1^2 + x_2^2 + L^2)}{8L^2 \lambda_2^f} \right]. \quad (\text{A21})$$

With this transformation, the matrix vector  $\mathbf{a}$  is mapped to

$$\mathbf{a} \rightarrow \hat{\mathbf{e}}_1 \left[ \frac{eB_3 x_2}{2c} + \frac{\hbar x_2 \sigma_3}{4\lambda_1^c \lambda_2^c} - \frac{\hbar}{8L^2} \left( \frac{2x_1 x_2 \sigma_1}{\lambda_2^f} + \frac{(3x_2^2 + x_1^2 - L^2)\sigma_2}{\lambda_1^f} \right) \right] - \hat{\mathbf{e}}_2 \left[ \frac{eB_3 x_1}{2c} + \frac{\hbar x_1 \sigma_3}{4\lambda_1^c \lambda_2^c} - \frac{\hbar}{8L^2} \left( \frac{2x_1 x_2 \sigma_2}{\lambda_1^f} + \frac{(3x_1^2 + x_2^2 - L^2)\sigma_1}{\lambda_2^f} \right) \right]. \quad (\text{A22})$$

Comparing Eqs. (A22) and (A14), we immediately conclude that with a non-uniform spin-orbit scattering strength of the form (49) with  $\lambda^f = \lambda_1^f = \lambda_2^f$  one should make the identification

$$a^2 = \left( \frac{L^2}{4(\lambda^f)^2} \right) \frac{v_F l \pi}{12L^2 \Delta}. \quad (\text{A23})$$

In terms of the energy scale  $\varepsilon_{\parallel}^{\text{so}}$ , this implies

$$\varepsilon_{\parallel}^{\text{so}} = \frac{1}{6} E_{\text{Th}} \left( \frac{L^2}{4(\lambda^f)^2} \right), \quad (\text{A24})$$

in agreement with the general relation (52).

<sup>1</sup> C. W. J. Beenakker and H. van Houten, *Solid State Phys.* **44**, 1 (1991).

<sup>2</sup> S. Hikami, A. I. Larkin, and Y. Nagaoka, *Prog. Theor. Phys.* **63**, 707 (1980).

<sup>3</sup> G. Bergmann, *Phys. Rep.* **107**, 1 (1984).

<sup>4</sup> A. V. Khaetskii and Yu. V. Nazarov, *Phys. Rev. B* **61**, 012639 (2000).

<sup>5</sup> J. A. Folk, S. R. Patel, K. M. Birnbaum, C. M. Marcus, C. I. Duruöz, and J. S. Harris, Jr., *Phys. Rev. Lett.* **86**, 2102 (2001).

<sup>6</sup> B. I. Halperin, A. Stern, Y. Oreg, J. N. H. J. Cremers, J. A. Folk, and C. M. Marcus, *Phys. Rev. Lett.* **86**, 2106 (2001).

<sup>7</sup> I. L. Aleiner and V. I. Fal'ko, *Phys. Rev. Lett.* **87**, 256801 (2001); **89**, 079902(E) (2002).

<sup>8</sup> In conventional notation, the Hamiltonian is specified in

coordinates with respect to the  $\hat{x} = [100]$  and  $\hat{y} = [010]$  directions. Then, the spin-orbit part of the Hamiltonian takes the form

$$H_{\text{so}} = \frac{\gamma}{m} (p_x \sigma_y - p_y \sigma_x) + \frac{\eta}{m} (p_x \sigma_x - p_y \sigma_y).$$

Here  $\gamma$  and  $\eta$  are coupling constants for the Rashba and Dresselhaus terms, respectively. In terms of the rates  $\gamma$  and  $\eta$ , one has  $\hbar/2\lambda_1 = -\eta + \gamma$ ,  $\hbar/2\lambda_2 = -\eta - \gamma$ .

<sup>9</sup> Y. Meir, Y. Gefen, and O. Entin-Wohlman, *Phys. Rev. Lett.* **63**, 798 (1989).

<sup>10</sup> H. Mathur and A. D. Stone, *Phys. Rev. Lett.* **68**, 2964 (1992).

<sup>11</sup> Y. Oreg and O. Entin-Wohlman *Phys. Rev. B* **46**, 2393 (1992).

- <sup>12</sup> For reviews, see: C. W. J. Beenakker, Rev. Mod. Phys. **69**, 731 (1997) and Y. Alhassid, Rev. Mod. Phys. **72**, 895 (2000).
- <sup>13</sup> J. P. Lu, J. B. Yau, S. P. Shukla, M. Shayegan, L. Wissinger, U. Rössler, and R. Winkler, Phys. Rev. Lett. **81**, 1282 (1998).
- <sup>14</sup> J. B. Miller, D. M. Zumbühl, C. M. Marcus, Y. B. Lyanda-Geller, D. Goldhaber-Gordon, K. Campman, A. C. Gossard, Phys. Rev. Lett. **90**, 076807 (2003).
- <sup>15</sup> D. M. Zumbühl, J. B. Miller, C. M. Marcus, K. Campman, and A. C. Gossard, Phys. Rev. Lett. **89**, 276803 (2002).
- <sup>16</sup> P. W. Brouwer, J. N. H. J. Cremers, and B. I. Halperin, Phys. Rev. B **65**, 081302 (2002).
- <sup>17</sup> V. I. Fal'ko and T. Jungwirth, Phys. Rev. B **65**, 81306 (2002).
- <sup>18</sup> M.L. Mehta, *Random Matrices*, (Academic, New York, 1991).
- <sup>19</sup> P. W. Brouwer, K. M. Frahm, and C. W. J. Beenakker, Waves in Random Media **9**, 91 (1999) [cond-mat/9809022].
- <sup>20</sup> P. W. Brouwer and C. W. J. Beenakker, J. Math. Phys. **37**, 4904 (1996).
- <sup>21</sup> B. L. Altshuler and B. D. Simons in *Mesoscopic Quantum Physics*, E. Akkermans, G. Montambaux, J.-L. Pichard, and J. Zinn-Justin, eds, (North Holland, Amsterdam, 1995).
- <sup>22</sup> M. Büttiker, Phys. Rev. B **33**, 3020 (1986); IBM J. Res. Dev. **32**, 63 (1988).
- <sup>23</sup> H. U. Baranger and P. A. Mello, Phys. Rev. B **51**, 4703 (1995).
- <sup>24</sup> P. W. Brouwer and C. W. J. Beenakker, Phys. Rev. B **55**, 4695 (1997).
- <sup>25</sup> N. Argaman, Phys. Rev. Lett. **75**, 2750 (1995).
- <sup>26</sup> J. N. H. J. Cremers, Ph. D. thesis (Harvard, 2002).